

The Nature of the Chemical Bond Revisited: An Energy-Partitioning Analysis of Nonpolar Bonds

Attila Kovács,^[a, b] Catharine Esterhuysen,^[a, c] and Gernot Frenking*^[a]

Abstract: The nature of the chemical bond in nonpolar molecules has been investigated by energy-partitioning analysis (EPA) of the ADF program using DFT calculations. The EPA divides the bonding interactions into three major components, that is, the repulsive Pauli term, quasiclassical electrostatic interactions, and orbital interactions. The electrostatic and orbital terms are used to define the nature of the chemical bond. It is shown that nonpolar bonds between main-group elements of the first and higher octal rows of the periodic system, which are prototypical covalent bonds, have large attractive contributions from classical electrostatic interactions, which may even be stronger than the attractive orbital interactions. Fragments of molecules with totally symmetrical electron-density distributions, like the nitrogen atoms in N₂, may strongly attract each other through classical electrostatic forces, which constitute 30.0% of the total attractive interactions. The electrostatic attraction can be enhanced by anisotropic charge distribution of the valence electrons of the atoms that have local areas of (negative) charge

concentration. It is shown that the use of atomic partial charges in the analysis of the nature of the interatomic interactions may be misleading because they do not reveal the topography of the electronic charge distribution. Besides dinitrogen, four groups of molecules have been studied. The attractive binding interactions in H_nE–EH_n (E = Li to F; n = 0–3) have between 20.7 (E = F) and 58.4% (E = Be) electrostatic character. The substitution of hydrogen by fluorine does not lead to significant changes in the nature of the binding interactions in F_nE–EF_n (E = Be to O). The electrostatic contributions to the attractive interactions in F_nE–EF_n are between 29.8 (E = O) and 55.3% (E = Be). The fluorine substituents have a significant effect on the Pauli repulsion in the nitrogen and oxygen compounds. This explains why F₂N–NF₂ has a much weaker bond than H₂N–NH₂, whereas the interac-


tion energy in FO–OF is much stronger than in HO–OH. The orbital interactions make larger contributions to the double bonds in HB=BH, H₂C=CH₂, and HN=NH (between 59.9% in B₂H₂ and 65.4% in N₂H₂) than to the corresponding single bonds in H_nE–EH_n. The orbital term ΔE_{orb} (72.4%) makes an even greater contribution to the HC≡CH triple bond. The contribution of ΔE_{orb} to the H_nE–EH_n bond increases and the relative contribution of the π bonding decreases as E becomes more electronegative. The π-bonding interactions in HC≡CH amount to 44.4% of the total orbital interactions. The interaction energy in H₃E–EH₃ (E = C to Pb) decreases monotonically as the element E becomes heavier. The electrostatic contributions to the E–E bond increases from E = C (41.4%) to E = Sn (55.1%) but then decreases when E = Pb (51.7%). A true understanding of the strength and trends of the chemical bonds can only be achieved when the Pauli repulsion is considered. In an absolute sense the repulsive ΔE_{Pauli} term is in most cases the largest term in the EPA.

Keywords: bond theory • bonding analysis • chemical bonding • density functional calculations • energy-partitioning analysis

[a] Dr. A. Kovács, Dr. C. Esterhuysen, Prof. G. Frenking
Fachbereich Chemie, Philipps-Universität Marburg
Hans-Meerwein-Strasse, 35042 Marburg (Germany)
Fax: (+49) 6421-282-5566
E-mail: frenking@chemie.uni-marburg.de

[b] Dr. A. Kovács
Hungarian Academy of Sciences
Budapest University of Technology and Economics
Research Group of Technical Analytical Chemistry
1111 Budapest Szt. Gellért tér 4 (Hungary)

[c] Dr. C. Esterhuysen
Department of Chemistry, Stellenbosch University
Matieland, 7602 (South Africa)

 Supporting information for this article is available on the WWW under <http://www.chemeurj.org/> or from the author. Geometries in Z-matrix format and energies of the optimized structures.

Introduction

According to the classical view of chemical bonding, nonpolar bonds between identical fragments R in a molecule R–R are established through covalent interactions. The model of a covalent bond consisting of a pair of electrons shared between two atoms was introduced into chemistry by Lewis.^[1,2] This type of chemical bonding, which leads in most cases to an accumulation of the interatomic electronic charge,^[3] is conceptually different from ionic bonding which can be described in terms of the classical Coulombic attraction that arises when two charges of opposite sign attract each other. In modern terminology, covalent bonding is a result of interactions between shared electrons while ionic bonding arises from closed-shell interactions between separated fragments which carry opposite charges, that is, charged species whose electron densities do not overlap. Ionic bonding can be described by the laws of classical electrostatic interactions.

The understanding of covalent bonds in terms of the basic laws of physics puzzled scientists for a long time until quantum theory was developed and applied to chemical problems. Heitler and London showed in 1927 that the strongly attractive forces between two hydrogen atoms can only be understood when the electrons are described as wave functions, which are then used to express the electronic structure of H₂.^[4] Heitler and London called it a “characteristic quantum mechanical resonance phenomenon”, which is crucial for the understanding of the interactions between neutral atoms. It should be emphasized that covalent and ionic bonding are both the result of electrostatic forces. We would also like to point out that besides the electrostatic interactions the kinetic energy of the electrons is also very important for the chemical bond.^[5] The difference is that quantum theoretical laws enforce electrons to behave in a peculiar way when they interact, which can be understood by treating them as resonating waves which may lead to a strong attraction that yields chemical bonding. We would like to point out that the “resonance phenomenon”, known as orbital interactions in modern terminology, is not associated with the pairing of two electrons which Lewis believed to be the driving force for a covalent bond. Resonance of the wave function takes place when there is only one electron such as in H₂⁺.^[6]

Calculation of the quasiclassical^[7] electrostatic interactions, ΔE_{elstat} , between two hydrogen atoms at the equilibrium distance of H₂ (a so-called promolecule) indicates only a spurious attraction. Nearly all the bonding energy in dihydrogen comes from the resonating wave function. Since the wave function is usually described in terms of one-electron functions called molecular orbitals, the bonding in H₂ arises nearly exclusively from orbital interactions. This finding has led covalent interactions in nonpolar bonds to be described in many chemistry textbooks only in terms of molecular orbitals, that is, covalent bonding and orbital interactions are considered as synonymous. Polar bonds between different atoms or groups R–R' are then considered to have contributions from both covalent and ionic attractions. However, a

value of $\Delta E_{\text{elstat}} \sim 0$ for H₂ is atypical of nonpolar diatomic molecules! In 1986 Spackman and Maslen calculated the electrostatic energies of 148 polar and nonpolar diatomic compounds.^[8] They showed that the quasiclassical electrostatic attraction in 18 homoatomic species E₂, where E is an element up to the fourth row of the periodic table, is always very large except for H₂. The calculated values of ΔE_{elstat} were in most cases even larger than the bond dissociation energies! For example, the quasiclassical electrostatic attraction between two spherical nitrogen atoms in the ⁴S ground state at the equilibrium distance of N₂ was calculated to be $\Delta E_{\text{elstat}} = -330.7 \text{ kcal mol}^{-1}$ ^[8] while the bond dissociation energy (BDE) of dinitrogen is 228.5 kcal mol⁻¹.^[9] This is in striking contrast to H₂ which has a BDE of 109.6 kcal mol⁻¹^[9] but the calculated value for ΔE_{elstat} is only $-1.4 \text{ kcal mol}^{-1}$.^[8]

Spackman and Maslen were not the first to recognize that the quasiclassical Coulombic attraction in diatomic molecules E₂ is very large when E is not hydrogen. Hirshfeld and Rzotkiewicz reported as early as 1974 that the net electrostatic attraction makes a much larger contribution to the bonding of the heavier first-row E₂ molecules than to the bonding in H₂.^[10] The unusually weak electrostatic attraction in H₂ is a consequence of its small nuclear charge and the shape of the electronic charge cloud. The larger positive charge of the heavier nuclei results in a strong electrostatic attraction for the electrons of other neutral atoms at intermediate internuclear distances, which is contrary to the general belief that there are only weak electrostatic interactions between neutral atoms at equilibrium distance.

Several workers have pointed out that the quasiclassical electrostatic attraction in heavier nonpolar molecules is quite strong,^[6,11,12a] but this knowledge has not led to a change in the standard interpretation of the nature of the interatomic interactions in nonpolar bonds that is found in many chemistry textbooks. Very recently, Rioux carried out a survey of popular general chemistry textbooks and showed that none of them gives an accurate description of covalent bonding.^[13] In particular, the kinetic energy of the electrons, which plays a paradoxical role in the formation of the chemical bond, as shown by the pioneering work of Ruedenberg,^[14] is never mentioned. Furthermore, the role of electrostatic interactions is described incorrectly.

There are several reasons why the knowledge about the physical origin of the chemical bond that has been gained in recent decades^[6] has had little impact on the way covalent bonding is presented and explained in chemistry textbooks. One reason is that Lewis' bonding model,^[1] which received quantum-chemical brute-force support from Pauling,^[15] is deceptively easy to interpret in terms of classical electrostatic interactions. Many chemists have a strong tendency to judge the value of a bonding model more by its simplicity and ease of visualization than by its agreement with physical laws and quantum theoretical insights. This can be explained by consideration of the early attempts to rationalize chemical bonding prior to the advent of quantum theory, when a true understanding of the chemical bond based on the first

principles of physics was not possible. The heuristic models that were developed during this time were remarkably successful; not only were they used to rationalize experimental observations, they also served as helpful guidelines in the search for new compounds and novel reactions, making them very popular amongst the wider chemical community. The quantum theoretical explanation of chemical bonding, in which the wave function Ψ was introduced as the fundamental quantity for describing electrons, deterred chemists from accepting a theoretical interpretation of the chemical bond for a long time owing to its complicated mathematical derivation and, more importantly, because the results are difficult to cast into simple models. Although quantum theory quickly proved invaluable for understanding chemical bonding, for example, it allowed longstanding problems such as the triplet ground state of dioxygen^[16a] and the peculiar stability of aromatic compounds^[16b] to be solved, it was treated like an illegitimate child by orthodox chemistry practitioners for a long time. Organic chemists eventually accepted the wave function as a helpful quantity because pericyclic reactions could only be explained by MO arguments by using the symmetry of Ψ . The didactical approach and the use of simple figures, which were introduced by Woodward and Hoffmann in their ground-breaking work, were important reasons for the acceptance of the wave function.^[17]

This does not mean that we think it necessary to discard the heuristic bonding models that are so widely used in chemistry. What is required, however, is an interpretation of the models that is in agreement with the physical origin of the chemical bond. It is necessary to connect the historically derived bonding models with the knowledge of the interatomic interactions that has been gained through accurate quantum theoretical investigations. Quantum theoretical support for an empirical chemical heuristic model is important for two reasons: one learns where the limits of the model are to be expected and how the model can be extended so it is more reliable. With this paper we wish to contribute to this endeavour. The goal of this study was to quantitatively interpret the chemical bond in terms of quasiclassical electrostatic interactions, the Pauli repulsion, and orbital interactions through accurate quantum-chemical calculations. The relative strengths of the attractive contributions to chemical bonding, that is, the electrostatic, ΔE_{elstat} , and orbital, ΔE_{orb} , interactions, can then be used to classify and to compare chemical bonds.

Before starting, we wish to comment on the terms “ionic bonding” and “electrostatic interactions” to avoid confusion. The former term describes the attractive interactions between two ions that have opposite charges, which can be understood in terms of the classical electrostatic attraction between a positive and a negative charge. Thus, ionic bonding as it is found in ionic solids is largely the result of purely electrostatic interactions. However, electrostatic interactions do not automatically mean that there is ionic bonding. Nonpolar (covalent) bonds may also contain strong electrostatic attractions between the bonded atoms which can make a

larger contribution to the bonding than the orbital interactions. The change in the absolute and relative contributions of the orbital and electrostatic attractions on going from nonpolar to polar bonds is the topic of another paper.^[18]

In this paper we will first present the results of the bonding analysis of N_2 . The calculated value for the electrostatic attraction, ΔE_{elstat} , will be compared with the result reported by Spackman and Maslen.^[8] Spackman and Maslen write in their paper “A more detailed analysis of bonding in diatomics, in the spirit of that outlined by Morokuma and Kitaura, may well be warranted.” This is exactly what we report in this paper, although our analysis, however, extends beyond diatomic molecules. We have used the energy-partitioning analysis (EPA) of the ADF program,^[12] which is based on the methods of Morokuma^[19] and Ziegler and Rauk.^[20] After discussing the bonding analysis of N_2 we analyze the homolytic bonding between singly bonded elements of the first octal row of the periodic table $\text{H}_n\text{E}-\text{EH}_n$ ($\text{E}=\text{Li}$ to F), that is, of the nonpolar molecules Li_2 , $\text{HBe}-\text{BeH}$, $\text{H}_2\text{B}-\text{BH}_2$, $\text{H}_3\text{C}-\text{CH}_3$, $\text{H}_2\text{N}-\text{NH}_2$, $\text{HO}-\text{OH}$, and F_2 . We also investigate the changes in the nature of the $\text{E}-\text{E}$ bonds when hydrogen is substituted by fluorine, that is, in the molecules $\text{F}_n\text{E}-\text{EF}_n$ ($\text{E}=\text{Be}$ to O). In the third part we analyze the bonding interactions in the multiple bonds $\text{HB}=\text{BH}$, $\text{H}_2\text{C}=\text{CH}_2$, $\text{HC}=\text{CH}$, and $\text{HN}=\text{NH}$. In the final part of the study the $\text{H}_3\text{C}-\text{CH}_3$ bond in ethane is compared with the $\text{H}_3\text{E}-\text{EH}_3$ bond of the heavier Group 14 elements ($\text{E}=\text{Si}$ to Pb). The results suggest that the standard interpretation of nonpolar bonds, which considers only orbital interactions, should be modified. In addition to the Pauli repulsion, there are two attractive components, the orbital and quasiclassical electrostatic interactions, that contribute to the total interaction energy. The use of Kohn–Sham orbitals instead of Hartree–Fock orbitals has been justified by Baerends and co-workers.^[12,21]

This paper is a continuation of our systematic studies of the nature of the chemical bond. In previous studies we focussed on the bonding in donor–acceptor complexes, that is, the bonding interactions that take place between closed-shell fragments.^[22] We are presently studying the bonding interactions between open-shell fragments. We wish to point out that there are other workers in the field who have recently reported energy-partitioning analyses of chemical bonds.^[23]

Methods

The geometries of the molecules were optimized at the nonlocal DFT level of theory by using Becke’s exchange functional^[24a] in conjunction with Perdew’s correlation functional^[24b] (BP86). Uncontracted Slater-type orbitals (STOs) were employed as basis functions in SCF calculations.^[25a] Triple- ζ -quality basis sets were used, which were augmented by two sets of polarization functions, that is, p and d functions for the hydrogen atom and d and f functions for the other atoms. This level of theory is denoted as BP86/TZ2P. An auxiliary set of s, p, d, f, and g STOs was used to fit the molecular densities and to represent the Coulomb and exchange potentials accurately in each SCF cycle.^[25b] Scalar relativistic effects were considered by using the zero-order regular approximation (ZORA).^[26] All structures were verified as minima on the potential energy surface by

calculating the Hessian matrices. The atomic partial charges were calculated by using the Hirshfeld partitioning scheme.^[27] The calculations were carried out using the ADF(2.3) program package.^[12]

The $\text{N}\equiv\text{N}$, $\text{H}_n\text{E}-\text{EH}_n$, and $\text{F}_n\text{E}-\text{EF}_n$ binding interactions were analyzed by using the ADF energy-partitioning scheme^[12] which was originally developed by Morokuma^[19] and later modified by Ziegler and Rauk.^[20] The focus of the bonding analysis was the instantaneous interaction energy, ΔE_{int} , of the bond, which is the energy difference between the molecule and its fragments in the frozen geometry of the compound. The interaction energy can be divided into three main components [Eq. (1)],

$$\Delta E_{\text{int}} = \Delta E_{\text{elstat}} + \Delta E_{\text{Pauli}} + \Delta E_{\text{orb}} \quad (1)$$

where ΔE_{elstat} is the electrostatic interaction energy between the fragments and is calculated by using the frozen electron-density distribution of the N , EH_n or EF_n fragments in the $\text{N}\equiv\text{N}$, $\text{H}_n\text{E}-\text{EH}_n$ or $\text{F}_n\text{E}-\text{EF}_n$ molecules. The second term in Equation (1), ΔE_{Pauli} , refers to the repulsive interactions between the fragments, which are caused by the fact that two electrons with the same spin cannot occupy the same region in space. ΔE_{Pauli} is calculated by enforcing the Kohn–Sham determinant of the orbitals of the superimposed fragments to obey the Pauli principle by antisymmetrization and renormalization. The stabilizing orbital interaction term, ΔE_{orb} , which incorporates the Heitler–London resonance phenomenon^[4] and has additional contributions from polarization and relaxation, is calculated in the final step of the energy-partitioning analysis when the Kohn–Sham orbitals relax to their optimal form. This term can be further partitioned into contributions from the orbitals that belong to different irreducible representations of the point group of the interacting system. The interaction energy, ΔE_{int} , together with the term ΔE_{prep} , which is the energy necessary to promote the fragments from their equilibrium geometry to the geometry in the compounds, can be used to calculate the bond dissociation energy, D_e , [Eq. (2)].^[28] Further details of the energy-partitioning analysis can be found in the literature.^[12]

$$-D_e = \Delta E_{\text{prep}} + \Delta E_{\text{int}} \quad (2)$$

It is important to recognize the physical meaning and the relevance of the energy terms involved in the EPA, ΔE_{elstat} , ΔE_{Pauli} , and ΔE_{orb} , to avoid misinterpretation of the calculated numbers. In particular, we would like to point out that in the calculation of ΔE_{elstat} the electron-density distribution of the fragments is used without consideration of the polarization of the charge distribution that arises in chemical interactions. The polarization is only considered in the final step of the EPA, which means that stabilization due to polarization and relaxation is completely included in the ΔE_{orb} term. Thus, the calculated electrostatic interaction energy, ΔE_{elstat} , of the unpolarized fragments is not the same as the total potential energy change of bond formation because the final electron density differs from the electronic density that results from superposition of the two fragment densities. While the ΔE_{elstat} term contains only quasiclassical electrostatic interactions that arise from the frozen electron densities of the fragments, the ΔE_{orb} term contains electrostatic attractions that result from quantum interference, potential energy changes due to polarization and relaxation and kinetic energy contributions. The ΔE_{Pauli} term also contains potential energy contributions because electronic charge is moved from the area of overlap of the fragments to nearer the nuclei which actually lowers the energy. The increase in the total energy due to the ΔE_{Pauli} term comes from the kinetic energy of the electrons which is much higher when they are closer to the nuclei. This is why the ΔE_{Pauli} term is sometimes called kinetic repulsion.^[12]

EPA has been used in the past mainly for analyzing the interactions between closed-shell species. To the best of our knowledge, the method was extended to electron-pair bonding for the first time by Bickelhaupt et al.^[29]

Results

Dinitrogen bond $\text{N}\equiv\text{N}$: Table 1 gives the results of the energy-partitioning analysis (EPA) of the nitrogen–nitrogen bond with nitrogen atoms in the $1s^2 2s^2 2p_x^1 2p_y^1 2p_z^1$ (^4S)

Table 1. Energy decomposition analysis^[a] of the $\text{N}\equiv\text{N}$ bond in N_2 at the BP86/TZ2P level of theory.

	N_2
ΔE_{int}	−240.5
ΔE_{Pauli}	802.4
$\Delta E_{\text{elstat}}^{\text{[b]}}$	−312.9 (30.0%)
$\Delta E_{\text{orb}}^{\text{[b]}}$	−730.0 (70.0%)
$\Delta E_{\sigma}^{\text{[c]}}$	−479.8 (65.7%)
$\Delta E_{\pi}^{\text{[c]}}$	−250.3 (34.3%)
E–E bond length [\AA] ^[d]	1.102 (1.09768) ^[e]
$D_e^{\text{[d]}}$	240.5 (228.5) ^[e]
$D_0^{\text{[d]}}$	237.1 (225.0) ^[e]

[a] Energy values are given in kcal mol^{-1} . [b] The percentage values in parentheses give the contribution to the total attractive interactions $\Delta E_{\text{elstat}} + \Delta E_{\text{orb}}$. [c] The percentage values in parentheses give the contribution to the orbital interactions ΔE_{orb} . [d] The experimental values are given in parentheses. [e] Ref. [9].

ground state used as fragments. The calculated bond dissociation energy ($D_0 = 237.1 \text{ kcal mol}^{-1}$) is in satisfactory agreement with the experimental value ($D_0 = 225.0 \text{ kcal mol}^{-1}$).^[9] The theoretical bond energy gives, after correction for the ZPE contribution, a value of $\Delta E_{\text{int}} = -240.5 \text{ kcal mol}^{-1}$ for the interaction energy. Table 1 shows that the calculated quasiclassical electrostatic attraction ($\Delta E_{\text{elstat}} = -312.9 \text{ kcal mol}^{-1}$) is very similar to the value that was calculated by SM ($\Delta E_{\text{elstat}} = -330.7 \text{ kcal mol}^{-1}$).^[8] Thus, our EPA shows that the electrostatic attraction in the N_2 promolecule is larger than the BDE, in agreement with the previous calculation by SM.

Table 1 shows that the quantum theoretical energy contributions of the electrostatic interactions, that is, the Pauli repulsion ($\Delta E_{\text{Pauli}} = 802.4 \text{ kcal mol}^{-1}$) and the orbital term ($\Delta E_{\text{orb}} = -730.0 \text{ kcal mol}^{-1}$), have much higher absolute values than the quasiclassical electrostatic attraction. The sum of the attractive orbital and the repulsive Pauli terms is $+72.4 \text{ kcal mol}^{-1}$, that is, the quantum theoretically defined energies (which include the contribution of the kinetic energy of the electrons) in N_2 have a weakening effect on the electrostatic attraction at the equilibrium distance. This is in contrast to H_2 in which the bonding is exclusively derived from the orbital term, ΔE_{orb} . The energy-partitioning analysis of dihydrogen, using the same level of theory as used in this work, gives a repulsive electrostatic contribution of $\Delta E_{\text{elstat}} = 5.8 \text{ kcal mol}^{-1}$ at the equilibrium distance. The binding in H_2 is a result of orbital interactions only which give a stabilizing contribution of $-118.7 \text{ kcal mol}^{-1}$.^[30]

The large value for the quasiclassical electrostatic attraction in N_2 may come as a surprise to many chemists who assume that the attractive and repulsive interactions be-

tween the positively charged nuclei and the negatively charged electrons in dinitrogen, which has an overall charge of zero, should roughly cancel. A model calculation of the quasiclassical attraction in N_2 by Kutzelnigg gave a similar result.^[31] A pictorial explanation was given by Bickelhaupt and Baerends.^[32] When two atoms approach each other with spherical charge densities, the repulsion between the interpenetrating clouds is weaker than the repulsion between the point charges that are at the center of the charge. This is why the repulsive term between the electronic charges of the two atoms at intermediate distances is smaller than the two attractive terms (the attraction between the electrons of one atom and the nucleus of the other atom) and the repulsion between the nuclei. The net result is an overall charge attraction.

We analyzed the nitrogen–nitrogen interactions at different interatomic distances by using the EPA method. Figure 1 shows the energy curves for ΔE_{int} , ΔE_{elstat} , ΔE_{Pauli} , and ΔE_{orb} for N–N distances between 0.6 and 1.8 Å. From the calculations it can be predicted that, on the basis of the electrostatic interactions alone, the dinitrogen molecule would have a bond length of ~ 0.85 Å, with a value for ΔE_{elstat} of ~ 450 kcal mol⁻¹. Assuming that the virial theorem holds at this point (the molecular virial theorem for a stationary

system reads $\Delta E = 0.5\Delta V$ and $\Delta V = -\Delta T$, where V is the potential energy and T is the kinetic energy), the bond dissociation energy would be ~ 225 kcal mol⁻¹, which is close to the experimental value ($D_e = 228.5$ kcal mol⁻¹).^[9] Classical forces would yield nearly the same BDE for N_2 as was calculated by quantum theory, albeit at a significantly shorter bond length. Figure 1 shows that the curves for ΔE_{int} and ΔE_{elstat} cross at a N–N distance of ~ 1.3 Å. At shorter distances, the repulsive contributions of ΔE_{Pauli} are stronger than those of the attractive ΔE_{orb} term, but at longer N–N distances the latter interactions are stronger than the ΔE_{Pauli} term.

The two attractive energy contributions to the nitrogen–nitrogen bond are $\Delta E_{\text{elstat}} = -312.9$ kcal mol⁻¹ and $\Delta E_{\text{orb}} = -730.0$ kcal mol⁻¹. We have previously proposed that the ratio of the two attractive energy terms should be used to define the character of the bond in terms of electrostatic and orbital interactions.^[22] The calculated numbers suggest that the chemical bond in N_2 has 30.0% electrostatic character while 70.0% comes from orbital interactions. Note that these percentage values are the contribution to the attractive interactions and not to the total interactions. The breakdown of the ΔE_{orb} term into orbitals that belong to different irreducible representations of the $D_{\infty h}$ point group show that the contribution of the σ bond (-479.8 kcal mol⁻¹) is much larger than that of the degenerate π bond (-250.3 kcal mol⁻¹). This is in agreement with the general assessment that σ bonds are stronger than π bonds. However, Kutzelnigg concluded upon theoretical analysis of the overlapping orbitals of the N–N σ bond that the latter is already in the antibonding region.^[33] This is because the interatomic distance is very short. It was suggested that the σ bond is much weaker than the π bond,^[34] but this seems to be at variance with the values for ΔE_{σ} and ΔE_{π} determined by EPA, which are given in Table 1. However, these values refer only to the attractive interactions between electrons with opposite spins, while the repulsive interactions between electrons with the same spin are given by the ΔE_{Pauli} term. The latter cannot be divided into orbitals that have different symmetry but a comparison of the ΔE_{Pauli} value for N_2 (802.4 kcal mol⁻¹) with the much smaller value for C_2 (252.3 kcal mol⁻¹) suggests that the strong repulsion arises mainly from the electrons in the σ orbitals. Note that the 5s(HOMO) of N_2 is the LUMO orbital of C_2 ($X^1\Sigma_g^+$). The sum of the attractive (ΔE_{orb}) and repulsive (ΔE_{Pauli}) interactions of the electrons in the σ orbitals of dinitrogen contribute very little if anything to the N–N bond. Note also that the sum of ΔE_{orb} (-730.0 kcal mol⁻¹) and ΔE_{Pauli} (802.4 kcal mol⁻¹) results in a repulsive contribution to ΔE_{int} . According to the EPA, N_2 is a stable molecule only because of the strong contribution of the quasiclassical electrostatic interaction.

The results of the EPA of N_2 have shown that the electrostatic attractions between the spherical nitrogen atoms, which amount to 30.0% of the total attraction, make a significant contribution to the nonpolar bond between two elements of the first octal row. The data also show that the Pauli repulsion plays a very important role in the strength of the chemical bond. In the next section we investigate the

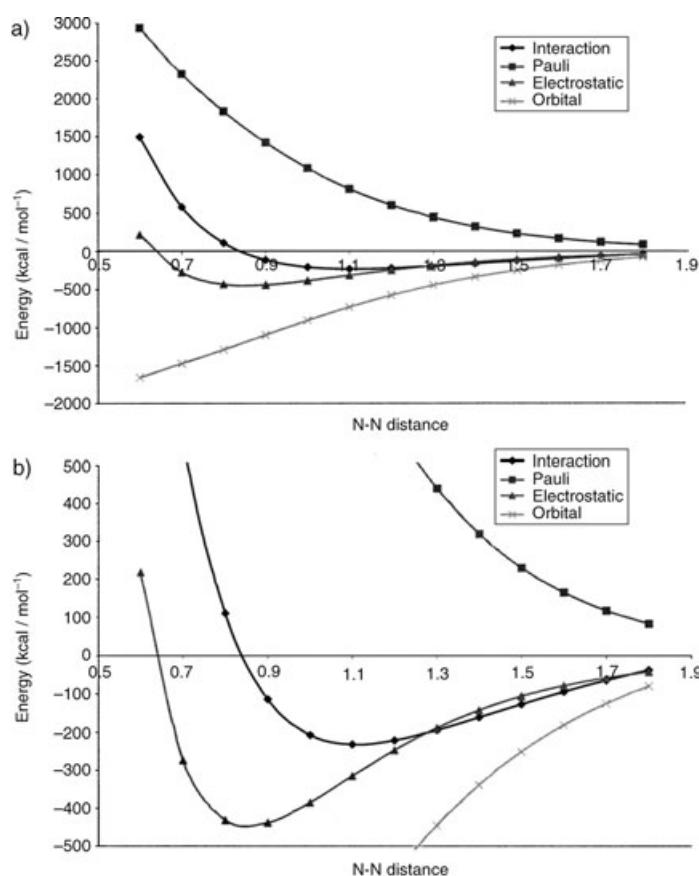


Figure 1. Energy contributions of ΔE_{elstat} , ΔE_{Pauli} and ΔE_{orb} to the total interaction energy ΔE_{int} in N_2 as a function of N–N interatomic distance: a) large scale; b) small scale.

differences in the nonpolar single bonds between atoms of the first octal row of the periodic system.

H_nE–EH_n bonds (E=Li to F; n=0–3): Table 2 gives the most important results from the EPA of the H_nE–EH_n bonds (E=Li to F) and the calculated bond lengths. The complete geometries are given in the Supporting Information. The theoretical geometries and bond dissociation energies are in good agreement with experimental data, except for the bond energy of F₂. The theoretical BDE for F₂ ($D_0=51.5$ kcal mol⁻¹) is clearly higher than the experimental value ($D_0=37.9$ kcal mol⁻¹).

The calculations indicate that the C–C bond of ethane has the largest interaction energy ($\Delta E_{\text{int}}=-114.8$ kcal mol⁻¹) of the E–E single bonds that were investigated in our study. The bond dissociation energy for ethane ($D_e=93.1$ kcal mol⁻¹) is significantly lower than the ΔE_{int} value because of the rather large preparation energy ($\Delta E_{\text{prep}}=21.7$ kcal mol⁻¹); CH₃ has a planar equilibrium structure, while the methyl groups in ethane have a pyramidal geometry. The ZPE-corrected bond dissociation energy ($D_0=83.4$ kcal mol⁻¹) is in reasonable agreement with the experimental value of 89.9 kcal mol⁻¹.

The breakdown of ΔE_{int} into the three energy terms provides the most important result. Table 2 shows that the electrostatic attraction, ΔE_{elstat} , is -130.9 kcal mol⁻¹, which is 41.4% of the total attractive energy, while the orbital term, ΔE_{orb} , contributes -185.5 kcal mol⁻¹ (58.6%). The EPA reveals that, like the nitrogen–nitrogen bond in N₂, the quasi-classical electrostatic attraction between the methyl groups in ethane is stronger than the total interaction energy. It should be emphasized that this result does not depend on the partitioning procedure that was used in the bonding analysis. The only arbitrary decision made was the choice of methyl fragments for the analysis of the C–C bond in ethane.

Table 2 shows that the electrostatic character of the E–E bond increases monotonically from F–F (20.7%) to HBe–

BeH (58.4%) but then decreases for Li–Li (37.3%). The absolute values of ΔE_{elstat} exhibit a less regular trend. There are several factors that determine the strength of the electrostatic attraction; the interatomic distance E–E, the nuclear charge of E and the topography of the electronic charge distribution. The latter can be visualized by analysis of the electron-density distribution. Figure 2a shows a contour line diagram of the Laplacian distribution of the electron density, $\nabla^2\rho(\mathbf{r})$, of the CH₃ fragment in the frozen geometry of ethane. The Laplacian distribution has been found to be a sensitive probe for the topology of the electron-density distribution, $\rho(\mathbf{r})$.^[40] The solid lines in Figure 2a show areas of relative electronic charge concentration, while the dashed

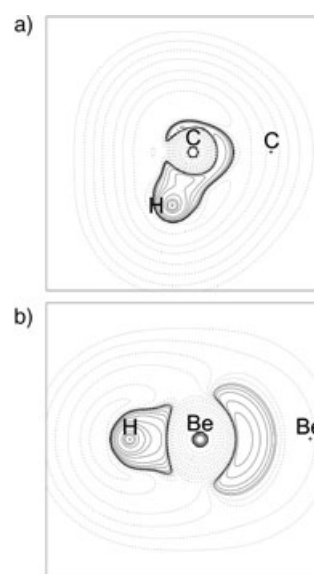


Figure 2. Contour line diagrams of the Laplacian distribution, $\nabla^2\rho(\mathbf{r})$, of a) CH₃ calculated with the frozen geometry of H₃C–CH₃ and b) BeH calculated with the frozen geometry of HBe–BeH. Solid lines give areas of charge concentration [$\nabla^2\rho(\mathbf{r}) < 0$], while dashed lines give areas of charge depletion [$\nabla^2\rho(\mathbf{r}) > 0$].

Table 2. Energy decomposition analysis^[a] of the H_nE–EH_n single bond (E=Li to F) at the BP86/TZ2P level of theory. Calculated atomic partial charges q_E and the E–E bond lengths are also given.

	Li ₂	Be ₂ H ₂	B ₂ H ₄	C ₂ H ₆	N ₂ H ₄	O ₂ H ₂	F ₂
Symm.	D_{orb}	D_{orb}	D_{2d}	D_{3d}	C_2	C_2	D_{orb}
ΔE_{int}	-20.6	-70.3	-114.5	-114.8	-76.8	-62.6	-52.8
ΔE_{pauli}	1.9	41.1	161.7	201.6	407.9	384.6	145.8
$\Delta E_{\text{elstat}}^{\text{[b]}}$	-8.4 (37.3%)	-65.1 (58.4%)	-140.5 (50.9%)	-130.9 (41.4%)	-178.3 (36.8%)	-145.8 (32.6%)	-41.1 (20.7%)
$\Delta E_{\text{orb}}^{\text{[b]}}$	-14.1 (62.7%)	-46.3 (41.6%)	-135.7 (49.1%)	-185.5 (58.6%)	-306.4 (63.2%)	-301.4 (67.4%)	-157.5 (79.3%)
$\Delta E_{\sigma}^{\text{[c]}}$	-14.1 (100%)	-46.3 (100%)	-119.7 (88.2%)	-175.5 (94.6%)			-151.3 (96.1%)
$\Delta E_{\pi}^{\text{[c]}}$			-16.0 (11.8%)	-10.0 (5.4%)			-6.2 (3.9%)
ΔE_{prep}	0	1.6	6.1	21.7	4.2	3.2	0
D_e	20.6	68.7	108.4	93.1	72.6	59.4	52.8
$D_0^{\text{[d]}}$	20.1 (26.4±1.0)	64.9 (71.7) ^[e]	103.0 (104.0) ^[e]	83.4 (89.9±0.5)	62.8 (65.8)	53.6 (50.9±1.0)	51.5 (37.9)
q_E [e]	0.0	0.196	0.081	-0.105	-0.214	-0.153	0.0
E–E [Å] ^[d]	2.737 (2.673)	2.101 (2.101) ^[f]	1.623 (1.656) ^[g]	1.532 (1.535)	1.443 (1.449)	1.473 (1.464) ^[h]	1.421 (1.412)

[a] Energy values are given in kcal mol⁻¹. [b] The percentage values in parentheses give the contribution to the total attractive interactions $\Delta E_{\text{elstat}}+\Delta E_{\text{orb}}$. [c] The percentage values in parentheses give the contribution to the orbital interactions ΔE_{orb} . [d] The experimental values are given in parentheses. Unless otherwise noted they have been taken from ref. [35]. [e] The theoretical value was taken from high-level (CBS-Q) ab initio calculations, see ref. [36]. [f] The theoretical value was taken from ref. [37]. [g] The theoretical value was taken from ref. [38]. [h] Ref. [39].

lines indicate areas of relative charge depletion. We would like to point out that the Laplacian distribution does not show absolute charge concentrations. It indicates rather the differences in the charge concentration around the atoms with respect to monotonous decay. In a separated atom, the Laplacian distribution gives the shell structure of the electron density. For a bonded atom in a molecule, the Laplacian distribution gives the deformation of the spherical charge distribution which is caused by the interatomic interactions. The shape of the Laplacian distribution of a molecule shows the areas of charge concentration and charge depletion relative to the charge distribution of the free atoms.

The shape of the Laplacian distribution in Figure 2a clearly shows that the carbon atom of the methyl group has an area of charge concentration that is aligned in the direction of the carbon–carbon bond of ethane. This charge concentration can be interpreted as the electron density of an electron in an sp^3 -hybridized orbital. The important point is that the carbon atom of the methyl radical in ethane has a highly anisotropic valence-electron distribution that enhances the electrostatic attraction with the nucleus of the other carbon atom. The EPA of the nitrogen–nitrogen bond in N_2 has shown, however, that fragments that have a spherically symmetrical charge distribution may strongly attract each other through classical electrostatic interactions. Hence, the anisotropy of the charge distribution enhances or weakens the ΔE_{elstat} term.

The electron-density distribution in the BeH fragment of HBe–BeH shows an even larger area of charge concentration at the beryllium atom directed towards the other Be (Figure 2b). This is because beryllium is less electronegative than carbon and thus the charge distribution is more diffuse. The charge distribution around the lithium atom is isotropic, however, because the valence electron occupies the 2s AO (Figure 3a). The results of the calculations suggest that the topography of the electron-density distribution of the interacting fragments is very important for the relative strength of the ΔE_{elstat} term. Note that according to the atomic partial charge, q_E , there should be electrostatic repulsion between the atoms in E–E. The repulsion should be particularly large for the N–N interactions in N_2H_4 , which actually has the biggest absolute value of the electrostatic attractions in the H_nE-EH_n molecules (Table 2). This is because only the total atomic net charge is considered in the partial charges, which can be misleading because the topography of the valence-electron distribution is neglected.

The EPA calculations underestimate the contribution of the electrostatic attraction. This can be demonstrated by further analysis of the electronic structure of Li_2 . Figure 3a exhibits the Laplacian distribution, $\nabla^2\rho(\mathbf{r})$, of lithium, which shows that an isotropic charge distribution, $\rho(\mathbf{r})$, is used to calculate ΔE_{elstat} . Figure 3b shows the Laplacian distribution of lithium in Li_2 , which was calculated by using the frozen orbital coefficients of lithium in the diatomic molecule. It is evident that the valence-electron concentration of lithium is highly polarized towards the other lithium atom as the charge concentration is aligned along the Li–Li bond. The

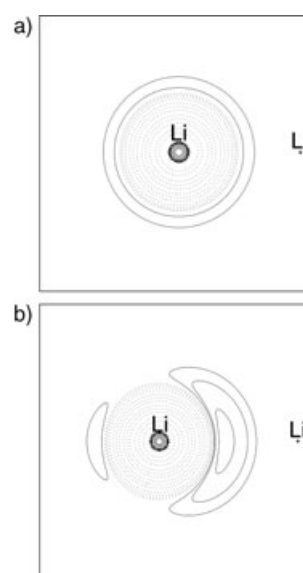


Figure 3. Contour line diagrams of the Laplacian distribution, $\nabla^2\rho(\mathbf{r})$, of a) the lithium atom calculated with complete SCF convergence and b) the lithium atom calculated with the frozen AO coefficients of Li_2 . The solid lines give areas of charge concentration [$\nabla^2\rho(\mathbf{r}) < 0$], while the dashed lines give areas of charge depletion [$\nabla^2\rho(\mathbf{r}) > 0$].

distorted electronic charge distribution of lithium will enhance the electrostatic attraction compared with the undistorted charge distribution because more negative charge is accumulated near the nucleus of the other lithium atom. It could be argued that ΔE_{elstat} should be calculated by using the electron-density distribution shown in Figure 3b. However, this would be meaningless because the distorted charge distribution, $\rho(\mathbf{r})$, is a result of all the interatomic interactions including the orbital interactions.

So far in the discussion of the nature of the chemical bond in H_nE-EH_n , we have focussed on the attractive energy contributions, ΔE_{orb} and ΔE_{elstat} , but the repulsive contribution of ΔE_{Pauli} is also very important for understanding the strength of the bonding interactions. For example, the calculated ΔE_{Pauli} value for H_2N-NH_2 is very large ($407.9 \text{ kcal mol}^{-1}$), which is why the ΔE_{int} value and the bond dissociation energy, D_e , are significantly lower than those of H_2B-BH_2 and H_3C-CH_3 . The strong Pauli repulsion arises from the interaction between the lone-pair electrons of the nitrogen atoms in the lowest-lying *gauche* conformation of hydrazine shown in Figure 4a. The attractive terms, ΔE_{elstat} and ΔE_{orb} , of H_2N-NH_2 have the largest values of the H_nE-EH_n molecules, which indicates that the lower BDE of H_2N-NH_2 relative to H_3C-CH_3 is not caused by a weaker nitrogen–nitrogen attraction. The results of the EPA of H_2N-NH_2 and $H_2Be-BeH_2$ show that use of the net interaction energy, ΔE_{int} , and the bond dissociation energy, D_e , in a comparison of the nature of the chemical bonds may be misleading. These two molecules have very similar ΔE_{int} and D_e values, but the Pauli repulsion in H_2N-NH_2 is 10 times higher than in $H_2Be-BeH_2$. The Pauli repulsion in

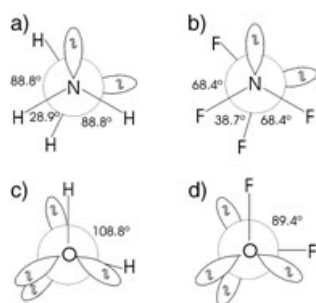


Figure 4. Sketch of the calculated conformations of a) H₂N-NH₂, b) F₂N-NF₂, c) HO-OH and d) FO-OF. The theoretically predicted torsion angles are given in degree.

HO-OH, which comes from the interatomic interactions of the oxygen lone-pair electrons (see Figure 4c), is also very large ($\Delta E_{\text{Pauli}} = 384.6 \text{ kcal mol}^{-1}$) and hence the reason for the rather low BDE.

The calculated energy terms of the fluorine-fluorine bond in F₂ are good examples with which to demonstrate the insight that has been gained through the EPA. It is well known that F₂ has a lower BDE than Cl₂. This is usually explained by the interatomic Pauli repulsion of the fluorine lone-pair electrons, which is expected to be rather strong owing to the short F-F interatomic distance. However, recent investigations of the chemical bonds in the dihalogen molecules X₂ (X=F to I) using the EPA method have shown that the small BDE of F₂ is in fact due to the unusually weak quasiclassical electrostatic attraction between the fluorine atoms.^[41] Fluorine is the most electronegative element and has a small atomic radius because of the compact electron-density distribution. Hence the electron density of the fluorine atom only overlaps with the nucleus of the other fluorine atom to a small extent.

It seems possible that the much weaker bond of F₂ ($\Delta E_{\text{int}} = -52.8 \text{ kcal mol}^{-1}$) relative to that of H₂B-BH₂ ($\Delta E_{\text{int}} = -114.5 \text{ kcal mol}^{-1}$) can also be explained by the difference between the ΔE_{elstat} values. Alternatively F₂ may have a weaker bond than H₂B-BH₂ because the former has a larger Pauli repulsion due to its lone-pair electrons which the latter does not have. The data in Table 2 does not support this reasoning. Comparison of the results for F₂ and H₂B-BH₂ shows that the orbital interactions in difluorine ($\Delta E_{\text{orb}} = -157.5 \text{ kcal mol}^{-1}$) are stronger than those in H₂B-BH₂ and that the Pauli repulsion ($\Delta E_{\text{Pauli}} = 145.8 \text{ kcal mol}^{-1}$) is weaker. The weaker bond of F₂ compared with H₂B-BH₂ is therefore a result of the significantly weaker electrostatic attraction (ΔE_{elstat}

$= -41.1 \text{ kcal mol}^{-1}$). The low ΔE_{elstat} value can be attributed to the compact 2p orbital of the most electronegative element, fluorine, which prevents a strong attraction between the unpaired electron in the 2p(σ) AO of one fluorine atom and the nucleus of the other. The same argument explains why the Pauli repulsion in F₂ is much weaker than that in HO-OH and H₂N-NH₂.

Table 2 also includes the σ and π contributions to the E-E orbital interactions in molecules that possess a mirror plane. The π -bonding contributions to ΔE_{orb} in B₂H₄, C₂H₆ and F₂ are, as expected, rather small. The strength of the hyperconjugative interactions in H₂B-BH₂ (D_{2d}) is $16.0 \text{ kcal mol}^{-1}$, which is 11.8% of the total ΔE_{int} term. This means that the empty p(π) orbital of boron is stabilized by one B-H bond by $4.0 \text{ kcal mol}^{-1}$. A detailed EPA of the boron-boron bond in X₂B-BX₂ (X=H, F, Cl, Br, and I) has been presented somewhere else.^[221]

F_nE-EF_n bonds (E=Be to O; n=1-3): We analyzed the E-E bonding in molecules of FBe-BeF, F₂B-BF₂, F₃C-CF₃, F₂N-NF₂, and FO-OF by the EPA method in order to learn about the effect of fluorine substitution on the nature of the bond. The results are given in Table 3.

The results of the EPA show that the ratio of the contribution of electrostatic and orbital interactions to the E-E bond does not change much when hydrogen is substituted by fluorine. The relative contributions of the electrostatic attraction to the binding interactions in F_nE-EF_n are as high as in H_nE-EH_n. In the former compounds the ΔE_{elstat} term constitutes between 29.8 (E=O) and 55.3% (E=Be) of the attractive interactions. Previous theoretical studies have indicated that several of the properties of these molecules change very little when hydrogen atoms are replaced by fluorine atoms.^[47] However, there are surprising differences in the bond strengths of F_nE-EF_n and H_nE-EH_n, which will be analyzed with the help of the EPA data.

Comparison of the calculated interaction energy values ΔE_{int} of the F_nE-EF_n bond (Table 3) with the ΔE_{int} values of

Table 3. Energy decomposition analysis^[a] of the F_nE-EF_n single bond (E=Be to O) at the BP86/TZ2P level of theory. Calculated atomic partial charges q_E and the E-E bond lengths are also given.

	Be ₂ F ₂	B ₂ F ₄	C ₂ F ₆	N ₂ F ₄	O ₂ F ₂
Symm.	<i>D_{∞h}</i>	<i>D_{2d}</i>	<i>D_{3d}</i>	<i>C₂</i>	<i>C₂</i>
ΔE_{int}	-71.8	-102.6	-92.9	-21.7	-97.6
ΔE_{Pauli}	26.3	123.8	253.9	323.1	614.4
ΔE_{elstat} ^[b]	-54.2 (55.3%)	-116.5 (51.5%)	-150.2 (43.4%)	-130.6 (37.9%)	-212.0 (29.8%)
ΔE_{orb} ^[b]	-43.9 (44.7%)	-109.9 (48.5%)	-196.6 (56.6%)	-214.2 (62.1%)	-500.0 (70.2%)
ΔE_{σ} ^[c]	-43.8 (99.8%)	-105.3 (95.8%)	-184.2 (93.7%)		
ΔE_{π} ^[c]	-0.1 (0.2%)	-4.6 (4.2%)	-12.4 (6.3%)		
ΔE_{prep}	1.3	4.1	5.6	4.6	36.0
D_e	70.5	98.5	87.3	17.1	61.6
D_0 ^[d]	68.4	95.2	84.3 (96.9 ± 2) ^[e]	14.2 (21 ± 1) ^[e]	59.2 (48) ^[f]
q_E [e]	0.268	0.247	0.221	0.113	0.159
E-E [Å] ^[d]	2.050	1.725 (1.719) ^[g]	1.567 (1.545) ^[h]	1.527 (1.492) ^[i]	1.204 (1.217) ^[j]

[a] Energy values in kcal mol⁻¹. [b] The percentage values in parentheses give the contribution to the total attractive interactions $\Delta E_{\text{elstat}} + \Delta E_{\text{orb}}$. [c] The percentage values in parentheses give the contribution to the orbital interactions ΔE_{orb} . [d] The experimental values are given in parentheses. [e] Ref. [42]. [f] On the basis of the heats of formation of FOOF and OF, which are reported in ref. [43]. [g] Ref. [44]. [h] Ref. [35]. [i] Ref. [45]. [j] Ref. [46].

the respective hydrogen-substituted analogues H_nE-EH_n (Table 2) shows that the fluorine atom has a non-uniform effect on the interaction energies. $FBe-BeF$ and $HBe-BeH$ have nearly the same ΔE_{int} values, whereas the fluorine analogues, F_2B-BF_2 and F_3C-CF_3 , have smaller interaction energies than the corresponding hydrogen systems. The interaction energy of N_2F_4 ($\Delta E_{int} = -21.7 \text{ kcal mol}^{-1}$) is much smaller than that of N_2H_4 ($\Delta E_{int} = -76.8 \text{ kcal mol}^{-1}$), while O_2F_2 ($\Delta E_{int} = -97.6 \text{ kcal mol}^{-1}$) has a significantly larger interaction energy than O_2H_2 ($\Delta E_{int} = -62.6 \text{ kcal mol}^{-1}$). The analysis of the energy terms should enable a better understanding of the peculiar trend of the calculated ΔE_{int} values.

Inspection of the energy contributions to ΔE_{int} of $FBe-BeF$ (Table 3) shows that the absolute values of ΔE_{elstat} , ΔE_{Pauli} , and ΔE_{orb} are smaller than those of $HBe-BeH$ (Table 2) even though the former compound has a shorter Be-Be bond than the latter. The $FBe-BeF$ bonding orbital has a higher percentage s character and is therefore more compact than the $HBe-BeH$ s orbital because fluorine is more electronegative than hydrogen.^[48] The repulsive and attractive beryllium-beryllium interactions in $FBe-BeF$ are therefore weaker than those in $HBe-BeH$ but the sum of the energy contributions in the two molecules yields nearly the same ΔE_{int} value. Note that the B-B distance in F_2B-BF_2 is significantly longer (1.725 Å) than that in H_2B-BH_2 (1.623 Å), which is in contrast to the findings with the beryllium system in which the substitution of hydrogen by fluorine causes a shortening of the central bond. This can be explained by consideration of the π -bonding contribution to the D_{2d} equilibrium structures of F_2B-BF_2 and H_2B-BH_2 . The B-H bonding orbital is a better hyperconjugative donor than the B-F bonding orbital. The latter orbitals contribute only $4.6 \text{ kcal mol}^{-1}$ to the B-B bond (Table 3) while the π -bonding contribution to the B-H bonds is $16.0 \text{ kcal mol}^{-1}$ (Table 2). The F_2B-BF_2 bond becomes shorter than the H_2B-BH_2 bond when the hyperconjugative interactions are turned off. Geometry optimization of planar (D_{2h}) structures gives bond lengths of 1.734 Å (F_2B-BF_2) and 1.752 Å (H_2B-BH_2). Hence, the $HBe-BeH$ and $FBe-BeF$ bonding interactions are mainly determined by direct Be-Be contact while the F_2B-BF_2 and H_2B-BH_2 bonding interactions in the D_{2d} equilibrium structures are significantly influenced by the hydrogen and fluorine substituents.

The interaction energy of F_3C-CF_3 ($\Delta E_{int} = -92.9 \text{ kcal mol}^{-1}$) is clearly smaller than that of H_3C-CH_3 ($\Delta E_{int} = -114.8 \text{ kcal mol}^{-1}$) even though the electrostatic attraction and orbital interactions in the former compound are stronger than in the latter. The smaller ΔE_{int} value for the former molecule can be explained in terms of the much higher Pauli repulsion in F_3C-CF_3 , which is caused by the fluorine's lone-pair electrons. Note that the bond dissociation energy of F_3C-CF_3 (calculated $D_0 = 84.3 \text{ kcal mol}^{-1}$; experimental $D_0 = 96.9 \text{ kcal mol}^{-1}$) is greater than that of H_3C-CH_3 (calculated $D_0 = 83.4 \text{ kcal mol}^{-1}$; experimental $D_0 = 89.9 \text{ kcal mol}^{-1}$). Two factors are responsible for this. One factor is significantly smaller preparation energy of the CF_3 groups ($\Delta E_{prep} = 5.6 \text{ kcal mol}^{-1}$) compared with that of the CH_3

groups ($\Delta E_{prep} = 21.7 \text{ kcal mol}^{-1}$). The second factor that leads to the higher bond dissociation energy of F_3C-CF_3 is the smaller contribution of the zero-point vibrational energy ($3.0 \text{ kcal mol}^{-1}$) compared with that for H_3C-CH_3 ($9.7 \text{ kcal mol}^{-1}$). The contributions of the π bonding to the ΔE_{orb} of F_3C-CF_3 ($-12.4 \text{ kcal mol}^{-1}$) and H_3C-CH_3 ($-10.0 \text{ kcal mol}^{-1}$) are similar although this property only plays a minor role in the C-C bond of these molecules.

The energy-partitioning analysis of F_2N-NF_2 was carried out by using the *gauche* conformation of the molecule (Figure 4b) in order to compare the results with those for the hydrazine molecule, which has a *gauche* equilibrium geometry. A recent experimental study of the conformational stability of N_2F_4 by Raman spectroscopy showed that the *gauche* and *trans* conformations are energetically nearly degenerate.^[49] The enthalpy difference was determined to be $0.197 \pm 0.017 \text{ kcal mol}^{-1}$ with the *trans* conformer the most stable rotamer.

F_2N-NF_2 has the smallest ΔE_{int} value ($-21.7 \text{ kcal mol}^{-1}$) of the F_nE-EF_n compounds (Table 3). Comparison of the energy components of the N-N bond in F_2N-NF_2 with those in H_2N-NH_2 (Table 2) shows that the absolute values of ΔE_{Pauli} , ΔE_{elstat} , and ΔE_{orb} in the former compound are smaller than those in the latter. This appears reasonable because F_2N-NF_2 has a significantly longer N-N bond (1.527 Å) than H_2N-NH_2 (1.443 Å). Shortening of the F_2N-NF_2 distance would result in a steep increase in the Pauli repulsion because the lone pairs on the fluorine atoms of the adjacent NF_2 groups would be closer to each other. Note, however, that F_3C-CF_3 also has a longer central bond than H_3C-CH_3 , and yet the former compound has larger values of ΔE_{Pauli} , ΔE_{elstat} , and ΔE_{orb} than the latter. The differences between the carbon and nitrogen systems can be explained by the shorter E-E bond length of H_2N-NH_2 (1.443 Å) relative to that of H_3C-CH_3 (1.532 Å) and by the lone pairs in the former compound, which also yield a strong Pauli repulsion in the hydrogen-substituted compound.

The most surprising result of the energy analysis of the F_nE-EF_n compounds is the very strong interaction energy of $FO-OF$ ($\Delta E_{int} = -97.6 \text{ kcal mol}^{-1}$). The calculated bond dissociation energy ($D_e = 61.6 \text{ kcal mol}^{-1}$) is much smaller than the ΔE_{int} value because the preparation energy of the OF fragments is rather high. The O-F distance in $FO-OF$ is clearly longer (1.608 Å) than that in free OF (1.366 Å). The lengthening of the O-F distance on formation of $FO-OF$ is in agreement with the experimental^[46] and previous theoretical^[50] results. Inspection of the energy terms (Table 3) shows that the contribution of the orbital interactions to the oxygen-oxygen bond is very large ($\Delta E_{orb} = -500.0 \text{ kcal mol}^{-1}$). The large value of the ΔE_{orb} term relative to that for $HO-OH$ compensates for the greater Pauli repulsion ($614.4 \text{ kcal mol}^{-1}$) in $FO-OF$. The O-O bond length in $FO-OF$ is much shorter (1.204 Å) than that in $HO-OH$ (1.473 Å). It is striking that substitution of the hydrogen atoms in H_3C-CH_3 and H_2N-NH_2 by fluorine leads to longer interatomic distances and smaller interaction energies for the central C-C and N-N bonds, while the central bond

length in FO–OF is much shorter and the ΔE_{int} value is significantly higher than for HO–OH. This can be explained in terms of the Pauli repulsion between the fluorine's lone-pair electrons in FO–OF, which can be reduced by rotation about the O–O bond (Figure 4d). This is not possible in $\text{F}_3\text{C–CF}_3$ and $\text{F}_2\text{N–NF}_2$ because any rotation about the C–C or N–N bond that reduces the Pauli repulsion between one pair of adjacent fluorine atoms will enhance the Pauli repulsion between other fluorine atoms (see Figure 4b for $\text{F}_2\text{N–NF}_2$). Note that the calculated FO–OF dihedral angle is 89.4° (experimental value 87.5°),^[46] which shows that the molecule tries to minimize the F–F repulsion in the *gauche* conformation. The Pauli repulsion between the fluorine atoms would be even weaker in the *trans* conformer, but then the favorable hyperconjugation between the oxygen's lone-pair electrons and the *trans* O–F σ^* orbitals would be lost.

Multiple bonds in HB=BH, $\text{H}_2\text{C=CH}_2$, $\text{HC}\equiv\text{CH}$, and $\text{HN}=\text{NH}$: We analyzed the double bonds between elements of the first octal row in the homopolar molecules HB=BH, $\text{H}_2\text{C=CH}_2$, and the *trans* form of HN=NH . The calculations on the boron species B_2H_2 were performed on the ($^1\Sigma_g^+$) singlet state ($D_{\infty h}$ symmetry), which is an excited state, because we wanted to compare the strength of the boron–boron π bond with the other molecules: B_2H_2 has a ($^3\Sigma_g^-$) triplet ground state.^[51] We also investigated the triple bond in acetylene, $\text{HC}\equiv\text{CH}$. The EPA results are given in Table 4.

The contributions of the electrostatic attraction to the binding interactions of the multiple bonds are smaller than

in the respective single bonds (Table 2) but they are still rather large. The $\text{H}_n\text{E=EH}_n$ double bonds possess between 34.6 (E=N) and 40.1% (E=B) electrostatic character. Thus, more than one third of the total interatomic attraction comes from electrostatic forces. The contribution of ΔE_{elstat} to the binding interactions of $\text{HC}\equiv\text{CH}$ is still 27.6%.

The calculated HB=BH bond length is clearly shorter (1.526 Å) than that of $\text{H}_2\text{B–BH}_2$ (1.623 Å) and the estimated interaction energy of the former compound ($\Delta E_{\text{int}} = -159.8 \text{ kcal mol}^{-1}$) is significantly larger than that of the latter ($\Delta E_{\text{int}} = -114.5 \text{ kcal mol}^{-1}$). How much of the increase in ΔE_{int} can be attributed to the boron–boron π bond? The results in Table 4 show that the contribution of ΔE_{orb} to the HB=BH bond is larger (absolute value: $-165.5 \text{ kcal mol}^{-1}$; relative value 59.9%) than the contribution of ΔE_{orb} to the $\text{H}_2\text{B–BH}_2$ bond. However, the σ contribution to ΔE_{orb} of HB=BH is actually less ($\Delta E_{\sigma} = -111.1 \text{ kcal mol}^{-1}$) than that to ΔE_{orb} of $\text{H}_2\text{B–BH}_2$ ($\Delta E_{\sigma} = -119.7 \text{ kcal mol}^{-1}$). This means that the π -bonding interactions in HB=BH lead to a reduction in the σ -bond strength, which is compensated by the enhanced π -bond strength. Table 4 shows that ΔE_{π} contributes $-54.4 \text{ kcal mol}^{-1}$ (32.9%) to ΔE_{orb} while ΔE_{σ} contributes $-111.1 \text{ kcal mol}^{-1}$ (67.1%). It follows that the π bond in HB=BH is half as strong as the σ bond. The electrostatic attraction and the Pauli repulsion in HB=BH are clearly weaker than in $\text{H}_2\text{B–BH}_2$.

The interaction energy in ethylene is also higher ($\Delta E_{\text{int}} = -191.1 \text{ kcal mol}^{-1}$) than in ethane ($\Delta E_{\text{int}} = -114.8 \text{ kcal mol}^{-1}$), but in contrast to the boron systems all the energy components of the doubly bonded molecule are larger than those of the singly bonded species. The contribution of the orbital interactions to the carbon=carbon double bond in ethylene is slightly larger (61.6%) than to the carbon–carbon single bond in ethane (58.6%). The π -bond strength in $\text{H}_2\text{C=CH}_2$ ($\Delta E_{\pi} = -79.2 \text{ kcal mol}^{-1}$) amounts to 27.2% of the total orbital interactions, while the σ contribution ($\Delta E_{\sigma} = -212.2 \text{ kcal mol}^{-1}$) is 72.8% of ΔE_{orb} . This means that the π -bond strength in ethylene has approximately one third the strength of the σ bond.

We wish to point out that the EPA of ΔE_{int} gives a much more direct estimate of the π -bond strength than the calculation or the measurement of the rotational barrier of the molecule since rotation about a double bond also affects the other energy components of the chemical bond, that is, the σ bonding, electrostatic attraction, and nuclear repulsion.

The data in Table 4 show that the N=N interaction energy of *trans*-diazene is also much higher ($\Delta E_{\text{int}} = -137.4 \text{ kcal mol}^{-1}$) than the N–N interaction energy of hydrazine ($\Delta E_{\text{int}} = -76.8 \text{ kcal mol}^{-1}$), but is clearly less than the ΔE_{int} value of ethylene. The absolute values of the energy components of HN=NH are significantly higher than those of ethylene, but the very strong Pauli repulsion in diazene ($\Delta E_{\text{Pauli}} = 599.4 \text{ kcal mol}^{-1}$) leads to a weaker net attraction. Note that the absolute values of the π -bonding interactions increase from HB=BH to $\text{H}_2\text{C=CH}_2$ and HN=NH , while the percentage ΔE_{π} decreases (Table 4).

Table 4. Energy decomposition analysis^[a] of the HB=BH, $\text{H}_2\text{C=CH}_2$, *trans*- HN=NH and $\text{HC}\equiv\text{CH}$ multiple bonds at the BP86/TZ2P level of theory. Calculated atomic partial charges q_E and the E–E bond lengths are also given.

	B_2H_2	C_2H_4	<i>trans</i> - N_2H_2	C_2H_2
Symm.	$D_{\infty h}$	D_{2h}	C_{2h}	$D_{\infty h}$
ΔE_{int}	-159.8	-191.1	-137.4	-280.0
ΔE_{Pauli}	116.3	281.9	599.4	255.4
$\Delta E_{\text{elstat}}^{\text{[b]}}$	-110.6	-181.6	-254.6	-147.5
	(40.1%)	(38.4%)	(34.6%)	(27.6%)
$\Delta E_{\text{orb}}^{\text{[b]}}$	-165.5	-291.4	-482.2	-387.9
	(59.9%)	(61.6%)	(65.4%)	(72.4%)
$\Delta E_{\sigma}^{\text{[c]}}$	-111.1	-212.2	-392.6	-215.5
	(67.1%)	(72.8%)	(81.4%)	(55.6%)
$\Delta E_{\pi}^{\text{[c]}}$	-54.4	-79.2	-89.6	-172.4
	(32.9%)	(27.2%)	(18.6%)	(44.4%)
ΔE_{prep}	4.4	12.9	5.6	32.8
D_e	155.4	178.2	131.8	247.2
$D_0^{\text{[d]}}$	149.8	168.3	123.7	238.7
		(175.4 ± 2)	(123.8 ± 1) ^[e]	(230.9 ± 2)
q_E [e]	0.031	-0.086	-0.106	-0.093
E–E	1.526	1.333	1.249	1.206
[Å] ^[d]	(1.498) ^[f]	(1.339)	(1.252) ^[g]	(1.203)

[a] Energy values are given in kcal mol^{-1} . [b] The percentage values in parentheses give the contribution to the total attractive interactions $\Delta E_{\text{elstat}} + \Delta E_{\text{orb}}$. [c] The percentage values in parentheses give the contribution to the orbital interactions ΔE_{orb} . [d] The experimental values are given in parentheses. Unless otherwise noted they have been taken from ref. [35]. [e] Ref. [52]. [f] The theoretical values was taken from ref. [53]. [g] Ref. [54].

The EPA results suggest (Table 4) that the much higher interaction energy of acetylene ($\Delta E_{\text{int}} = -280.0 \text{ kcal mol}^{-1}$) compared with that of ethylene ($\Delta E_{\text{int}} = -191.1 \text{ kcal mol}^{-1}$) comes from the increase in the strength of the orbital interactions. The electrostatic attraction in $\text{HC}\equiv\text{CH}$ ($\Delta E_{\text{elstst}} = -147.5 \text{ kcal mol}^{-1}$) is weaker than that in $\text{H}_2\text{C}=\text{CH}_2$ ($\Delta E_{\text{elstst}} = -181.6 \text{ kcal mol}^{-1}$), whereas the ΔE_{orb} value of the $\text{C}\equiv\text{C}$ triple bond ($-387.9 \text{ kcal mol}^{-1}$) is much higher than that of the double bond ($-291.4 \text{ kcal mol}^{-1}$). The increase in ΔE_{orb} is nearly exclusively a result of the π -bonding interactions in acetylene. The data in Table 4 indicate that the strength of the π bonding in $\text{HC}\equiv\text{CH}$ ($\Delta E_{\pi} = -172.4 \text{ kcal mol}^{-1}$) is much higher than in $\text{H}_2\text{C}=\text{CH}_2$ ($\Delta E_{\pi} = -79.2 \text{ kcal mol}^{-1}$), while the σ -bond strength in $\text{HC}\equiv\text{CH}$ ($\Delta E_{\sigma} = -215.5 \text{ kcal mol}^{-1}$) is nearly the same as in $\text{H}_2\text{C}=\text{CH}_2$ ($\Delta E_{\sigma} = -212.2 \text{ kcal mol}^{-1}$). This is not surprising because acetylene has a degenerate π orbital which has two components while the π orbital of ethylene has only one. The calculated data suggest that each of the π -orbital components of acetylene has about the same strength as the π orbital in ethylene. The π -bond strength in acetylene contributes 44.4% to the total orbital interactions.

Finally, we compare the $\text{C}\equiv\text{C}$ triple bond in acetylene with the triple bond in dinitrogen (Table 1). The calculated energy terms show that the triple bond in C_2H_2 has a significantly larger interaction energy than that in N_2 as a result of the much weaker Pauli repulsion in the former bond. The attractive interactions in the $\text{N}\equiv\text{N}$ bond ($\Delta E_{\text{elstst}} + \Delta E_{\text{orb}} = -1042.9 \text{ kcal mol}^{-1}$) are nearly twice as high as those in the $\text{HC}\equiv\text{CH}$ bond ($\Delta E_{\text{elstst}} + \Delta E_{\text{orb}} = -535.4 \text{ kcal mol}^{-1}$), although the difference between the ΔE_{Pauli} strengths is even greater.

$\text{H}_3\text{E}-\text{EH}_3$ bonds (E = C to Pb): We have also investigated the changes in the nature of the $\text{H}_3\text{E}-\text{EH}_3$ homopolar bonds along the Group 14 elements: E = C, Si, Ge, Sn, and Pb. Table 5 gives the results of the EPA.

The calculated data predict that the interaction energies ΔE_{int} decrease monotonically from the lightest member of the series $\text{H}_3\text{C}-\text{CH}_3$ ($\Delta E_{\text{int}} = -114.8 \text{ kcal mol}^{-1}$) to the heaviest $\text{H}_3\text{Pb}-\text{PbH}_3$ ($\Delta E_{\text{int}} = -48.2 \text{ kcal mol}^{-1}$). The dissociation energies, D_e and D_0 , display the same trend. With the exception of ethane, the absolute values of the interaction energies are only slightly larger than the D_e values because the preparation energies are rather small.

The electrostatic nature of the $\text{H}_3\text{E}-\text{EH}_3$ bond increases from E = C to E = Sn. The lead-lead bond has a slightly higher percentage contribution from the orbital interactions

Table 5. Energy decomposition analysis^[a] of the $\text{H}_3\text{E}-\text{EH}_3$ single bond (E = C to Pb) at the BP86/TZ2P level of theory. Calculated atomic partial charges q_E and E-E bond lengths are also given.

	C_2H_6	Si_2H_6	Ge_2H_6	Sn_2H_6	Pb_2H_6
Symm.	D_{3d}	D_{3d}	D_{3d}	D_{3d}	D_{3d}
ΔE_{int}	-114.8	-75.2	-69.7	-58.8	-48.2
ΔE_{Pauli}	201.6	101.2	114.4	98.3	84.0
$\Delta E_{\text{elstst}}^{\text{[b]}}$	-130.9 (41.4%)	-83.8 (47.5%)	-95.2 (51.7%)	-86.6 (55.1%)	-68.3 (51.7%)
$\Delta E_{\text{orb}}^{\text{[b]}}$	-185.5 (58.6%)	-92.6 (52.5%)	-88.9 (48.3%)	-70.5 (44.9%)	-63.9 (48.3%)
$\Delta E_{\sigma}^{\text{[c]}}$	-175.5 (94.6%)	-87.8 (94.8%)	-84.3 (94.8)	-67.5 (95.7%)	-61.2 (95.8)
$\Delta E_{\pi}^{\text{[c]}}$	-10.0 (5.4%)	-4.8 (5.2%)	-4.6 (5.2%)	-3.0 (4.3%)	-2.7 (4.2)
ΔE_{prep}	21.7	2.8	2.2	1.4	1.4
$D_e^{\text{[d]}}$	93.1	72.4	67.5	57.4(61.3) ^[e]	46.8
$D_0^{\text{[d]}}$	83.4 (89.9 ± 0.5) ^[f]	68.3 (74 ± 3) ^[g]	63.8 (70.2) ^[h]	54.4	43.6
q_E [e]	-0.105	0.208	0.184	0.263	0.250
E-E [\AA] ^[d]	1.532 (1.535) ^[f]	2.352 (2.331) ^[f]	2.418 (2.403) ^[f]	2.786 (2.758) ^[e]	2.898 (2.897) ^[i]

[a] Energy values in kcal mol^{-1} . [b] The percentage values in parentheses give the contribution to the total attractive interactions $\Delta E_{\text{elstst}} + \Delta E_{\text{orb}}$. [c] The percentage values in parentheses give the contribution to the orbital interactions ΔE_{orb} . [d] The experimental values are given in parentheses. [e] The theoretical value was taken from ref. [55]. [f] Ref. [35]. [g] Ref. [42]. [h] The theoretical value was taken from ref. [56]. [i] The theoretical value was taken from ref. [57].

than the tin-tin bond, which might be caused by relativistic effects which are particularly strong in lead compounds.^[58] Apart from this, the changes in the nature of the $\text{H}_3\text{E}-\text{EH}_3$ bond and the strengths of the energy terms along the series from carbon to lead are uniform. Note, however, that the absolute values of the Pauli repulsion and electrostatic attraction in $\text{H}_3\text{Ge}-\text{GeH}_3$ are larger than in $\text{H}_3\text{Si}-\text{SiH}_3$, possibly due to the filled 3d shell and the resulting contracted atomic radius of Ge relative to Si.

Summary

The interaction energy of a chemical bond can be meaningfully interpreted in terms of quasiclassical electrostatic interaction, Pauli repulsion, and orbital interactions. The contributions of all three terms must be considered when chemical bonds are compared. Chemical bonding is caused by classical electrostatic interactions and by the specific quantum mechanical kinematics of electrons, which result in the Pauli repulsion of occupied overlapping orbitals and the resonance and deformation of partially occupied orbitals.

The results of the EPA show that nonpolar covalent bonds between main-group elements of the first and higher octal rows of the periodic table have large contributions from quasiclassical electrostatic attractions between the bonded fragments that may be even stronger than orbital interactions. The bonding interactions in $\text{H}_n\text{E}-\text{EH}_n$ (E = Li to F; $n = 0-3$) possess between 20.7 (E = F) and 58.4% (E = Be) electrostatic character. The nature of the bonding interactions in H_2 , which comes exclusively from orbital interactions, is atypical of chemical bonds. The electrostatic bonding arises from the attraction between areas of electronic charge concentration in the valence-shell distribution of one atom and the nucleus of the other atom. With the exception of lithium, the electronic charge distribution in the valence shell of E in the fragment H_nE is highly anisotropic. Howev-

er, even fragments with a spherically symmetrical electronic charge distribution may strongly attract each other through quasiclassical electrostatic forces. This is evident from the calculated value $\Delta E_{\text{elstat}} = -312.9 \text{ kcal mol}^{-1}$ for N_2 . A true understanding of the nature of the chemical bond can only be achieved when the Pauli repulsion is considered. The binding interactions in $\text{H}_2\text{N}-\text{NH}_2$ and $\text{HO}-\text{OH}$ are weakened by strong Pauli repulsion.

The substitution of hydrogen by fluorine does not lead to significant changes in the nature of the binding interactions in $\text{F}_n\text{E}-\text{EF}_n$ ($\text{E} = \text{Be}$ to O), that is, the relative strengths of the orbital interactions and electrostatic attraction change little although the absolute values may change substantially. The fluorine substituents have a large effect on the Pauli repulsion in the nitrogen and oxygen compounds, which explains why $\text{F}_2\text{N}-\text{NF}_2$ has a much weaker bond than $\text{H}_2\text{N}-\text{NH}_2$, while the interaction energy in $\text{FO}-\text{OF}$ is much stronger than in $\text{HO}-\text{OH}$.

The double bonds in $\text{HB}=\text{BH}$, $\text{H}_2\text{C}=\text{CH}_2$, and $\text{HN}=\text{NH}$ have a higher degree of orbital interactions than the corresponding single bonds in $\text{H}_n\text{E}-\text{EH}_n$. Orbital interactions make an even bigger contribution to the covalent bonding in the $\text{HC}\equiv\text{CH}$ triple bond. The relative contribution of the ΔE_{elstat} term increases whilst that of the π bonding decreases as E becomes more electronegative. The π -bonding interactions in $\text{HC}\equiv\text{CH}$ amount to 44.4% of the total orbital interactions. The interaction energy in $\text{H}_3\text{E}-\text{EH}_3$ ($\text{E} = \text{C}$ to Pb) decreases monotonically as the element E becomes heavier. The electrostatic character of the $\text{E}-\text{E}$ bond increases from $\text{E} = \text{C}$ (41.4%) to $\text{E} = \text{Sn}$ (55.1%), but decreases when $\text{E} = \text{Pb}$ (51.7%).

Acknowledgements

We thank the referees whose constructive criticism helped to improve the manuscript. G.F. thanks Professor W.H.E. Schwarz for his helpful comments. This work was supported by a research grant from the Deutscher Akademischer Austauschdienst (DAAD). A.K. thanks the Joseph Eotvos Scholarship Foundation for a visiting fellowship. C.E. thanks the Alexander von Humboldt Foundation for a research fellowship. Additional funding was provided by the Deutsche Forschungsgemeinschaft and by the Fonds der Chemischen Industrie. Excellent service by the Hochschulrechenzentrum of the Philipps-Universität Marburg is gratefully acknowledged. Additional computer time was provided by the HLRS Stuttgart and HHLRZ Darmstadt.

- [1] a) G. N. Lewis, *J. Am. Chem. Soc.* **1916**, *38*, 762; b) G. N. Lewis, *Valence and the Structure of Atoms and Molecules*, American Chemical Society Monograph Series, New York, **1923**.
- [2] According to Mierzecki, the conception of the covalent bond was introduced by William Ramsey: R. Mierzecki, *The Historical Development of Chemical Concepts*, Kluwer Academic Publishers, Dordrecht, **1985**, p. 202. Lewis writes in his publication (ref. [1a]) that William Ramsay used very similar formulae to his in the book: *The Temple Primers; Modern Chemistry*.
- [3] We wish to point out that the accumulation of electronic charge in the bonding region is a result of chemical interactions but not the driving force. Also, as one referee pointed out, covalent interactions do not necessarily lead to an accumulation of the electronic charge in the bonding region. An example is the chemical bond in F_2 . The Laplacian distribution of the electron density shows depletion of electronic charge in the bonding region of F_2 . This was discussed by Cremer and Kraka who suggested that the energy density at the bond's critical point should be used as a sensitive probe for covalent bonding: D. Cremer, E. Kraka, *Angew. Chem.* **1984**, *96*, 612; *Angew. Chem. Int. Ed. Engl.* **1984**, *23*, 62. It is evident that energy is a more direct criterion for chemical bonding than charge distribution. Schwarz et al. have shown that an accumulation of electronic charge in the bonding region of F_2 is found when the differences between the electron density of F_2 and the properly arranged fluorine atoms is calculated: W. H. E. Schwarz, L. Mensching, K. Ruedenberg, L. L. Miller, P. Valtazanos, W. von Niessen, R. A. Jacobson, *Angew. Chem.* **1989**, *101*, 605; *Angew. Chem. Int. Ed. Engl.* **1989**, *28*, 597.
- [4] W. Heitler, F. London, *Z. Phys.* **1927**, *44*, 455.
- [5] The attractive part of the (covalent or ionic) chemical bonding results from the electrostatic forces derived from a nuclear-electron attraction. The counterpart of the electrostatic interactions is the kinetic energy. The kinetic energy, at the equilibrium distance, has a repulsive contribution whose absolute value is, according to the virial theorem, half the electrostatic attraction. This is discussed in refs. [6,10,11,13]. Our work focuses on and distinguishes between the electrostatic attraction, which is given by the quasiclassical term ΔE_{elstat} , and the orbital interaction (resonance) term, ΔE_{orb} .
- [6] A thorough discussion of previous work and the present understanding of the chemical bonding is given by: W. Kutzelnigg in *The Concept of the Chemical Bond* (Ed.: Z. B. Maksic), Springer, Berlin/Heidelberg, **1990**.
- [7] The term "quasiclassical" is used to indicate that the electron density ρ is calculated by using quantum theory but the interactions between the electrons and nuclei are calculated by assuming classical behaviour, that is, that no quantum interference takes place.
- [8] M. A. Spackman, E. N. Maslen, *J. Phys. Chem.* **1986**, *90*, 2020.
- [9] K. P. Huber, G. Herzberg, *Molecular Spectra and Molecular Structure IV. Constants of Diatomic Molecules*, Van Nostrand-Reinhold, New York, **1979**.
- [10] F. L. Hirshfeld, S. Rzotkiewicz, *Mol. Phys.* **1974**, *27*, 1319.
- [11] a) S. G. Wang, W. H. E. Schwarz, H. L. Lin, *Chem. Phys. Lett.* **1991**, *180*, 509; b) J. Autschbach, W. H. E. Schwarz, *J. Phys. Chem. A* **2000**, *104*, 6039.
- [12] a) F. M. Bickelhaupt, E. J. Baerends, *Rev. Comput. Chem.* **2000**, *15*, 1; b) G. te Velde, F. M. Bickelhaupt, E. J. Baerends, S. J. A. van Gisbergen, C. Fonseca Guerra, J. G. Snijders, T. Ziegler, *J. Comput. Chem.* **2001**, *22*, 931.
- [13] F. Rioux, *Chem. Educ.* **2003**, *8*, 1.
- [14] K. Ruedenberg, *Rev. Mod. Phys.* **1962**, *34*, 326.
- [15] L. Pauling, *The Nature of the Chemical Bond*, 3rd ed., Cornell University Press, Ithaca, New York, **1960**.
- [16] a) J. E. Lennard-Jones, *Trans. Faraday Soc.* **1929**, *25*, 668; b) E. Hückel, *Z. Phys.* **1931**, *70*, 204.
- [17] R. B. Woodward, R. Hoffmann, *The Conservation of Orbital Symmetry*, Verlag Chemie, Weinheim, **1970**.
- [18] C. Massera, G. Frenking, unpublished results.
- [19] K. Morokuma, *J. Chem. Phys.* **1971**, *55*, 1236.
- [20] a) T. Ziegler, A. Rauk, *Inorg. Chem.* **1979**, *18*, 1558; b) T. Ziegler, A. Rauk, *Inorg. Chem.* **1979**, *18*, 1755.
- [21] a) O. Gritsenko, P. Schipper, E. J. Baerends, *J. Chem. Phys.* **1997**, *107*, 5007; b) E. J. Baerends, O. Gritsenko, *J. Phys. Chem. A* **1997**, *101*, 5383; c) D. Chong, O. Gritsenko, E. J. Baerends, *J. Chem. Phys.* **2002**, *116*, 1760.
- [22] a) A. Diefenbach, F. M. Bickelhaupt, G. Frenking, *J. Am. Chem. Soc.* **2000**, *122*, 6449; b) J. Uddin, G. Frenking, *J. Am. Chem. Soc.* **2001**, *123*, 1683; c) Y. Chen, G. Frenking, *J. Chem. Soc., Dalton Trans.* **2001**, 434; d) M. Lein, J. Frunzke, A. Timoshkin, G. Frenking, *Chem. Eur. J.* **2001**, *7*, 4155; e) M. Doerr, G. Frenking, *Z. Allg. Anorg. Chem.* **2002**, *628*, 843; f) G. Frenking, K. Wichmann, N. Fröhlich, J. Grobe, W. Golla, D. Le Van, B. Krebs, M. Läge, *Organometallics* **2002**, *21*, 2921; g) J. Frunzke, M. Lein, G. Frenking, *Organometallics* **2002**, *21*, 3351; h) C. Loschen, K. Voigt, J. Frunzke, A. Diefenbach,

- M. Diedenhofen, G. Frenking, *Z. Allg. Anorg. Chem.* **2002**, 628, 1294; i) V. M. Rayón, G. Frenking, *Chem. Eur. J.* **2002**, 8, 4693; j) M. Cases, G. Frenking, M. Duran, M. Solà, *Organometallics* **2002**, 21, 4182; k) C. Esterhuysen, G. Frenking, *Theor. Chim. Acta* **2004**, 111, 381; l) M. Lein, A. Szabó, A. Kovács, G. Frenking, *Faraday Discuss.* **2003**, 124, 365; m) C. Esterhuysen, G. Frenking, *Chem. Eur. J.* **2003**, 9, 3518; n) G. Frenking, K. Wichmann, N. Fröhlich, C. Loschen, M. Lein, J. Frunzke, V. M. Rayón, *Coord. Chem. Rev.* **2003**, 238/239, 55.
- [23] a) F. M. Bickelhaupt, U. Radius, A. W. Ehlers, R. Hoffmann, E. J. Baerends, *New J. Chem.* **1998**, 22, 1; b) U. Radius, F. M. Bickelhaupt, A. W. Ehlers, N. Goldberg, R. Hoffmann, *Inorg. Chem.* **1998**, 37, 1080; c) A. W. Ehlers, E. J. Baerends, F. M. Bickelhaupt, U. Radius, *Chem. Eur. J.* **1998**, 4, 210; d) A. A. Dickinson, D. J. Willock, R. J. Calder, S. Aldridge, *Organometallics* **2002**, 21, 1146; e) L. E. Forslund, N. Kaltsoyannis, *New J. Chem.* **2003**, 27, 1108.
- [24] a) A. D. Becke, *Phys. Rev. A* **1988**, 38, 3098; b) J. P. Perdew, *Phys. Rev. B* **1986**, 33, 8822.
- [25] a) J. G. Snijders, E. J. Baerends, P. Vernooijs, *At. Nucl. Data Tables* **1982**, 26, 483; b) J. Krijn, E. J. Baerends, *Fit Functions in the HFS-Method*, Internal Report (in Dutch), Vrije Universiteit Amsterdam, The Netherlands, **1984**.
- [26] a) C. Chang, M. Pelissier, Ph. Durand, *Phys. Scr.* **1986**, 34, 394; b) J.-L. Heully, I. Lindgren, E. Lindroth, S. Lundquist, A.-M. Martensson-Pendrill, *J. Phys. B* **1986**, 19, 2799; c) E. van Lenthe, E. J. Baerends, J. G. Snijders, *J. Chem. Phys.* **1993**, 99, 4597; d) E. van Lenthe, E. J. Baerends, J. G. Snijders, *J. Chem. Phys.* **1996**, 105, 6505; e) E. van Lenthe, R. van Leeuwen, E. J. Baerends, J. G. Snijders, *Int. J. Quantum Chem.* **1996**, 57, 281.
- [27] E. L. Hirshfeld, *Theor. Chim. Acta* **1977**, 44, 129.
- [28] The preparation energy may also include electronic excitation energy if the electronic ground state of the fragment is different from the electronic reference state in the molecule. For example, the electronic reference state of the CH fragment in acetylene, HC≡CH, is the ($^4\Sigma^-$) quartet state but the electronic ground state is $^2\Pi$.
- [29] F. M. Bickelhaupt, N. M. M. Nibbering, E. M. van Wezenbeek, E. J. Baerends, *J. Phys. Chem.* **1992**, 96, 4864.
- [30] The EPA calculation of H₂ at the BP86/TZ2P level gives $\Delta E_{\text{orb}} = -99.6 \text{ kcal mol}^{-1}$ and $\Delta E_{\text{Pauli}} = -19.1 \text{ kcal mol}^{-1}$. The latter value is an artefact of the density functionals that were used. It is reasonable to add the unphysical ΔE_{Pauli} value to the orbital interaction term: F. M. Bickelhaupt, personal communication.
- [31] See ref. [6], p. 34.
- [32] See ref. [12a], p. 15.
- [33] W. Kutzelnigg, *Angew. Chem.* **1984**, 96, 262; *Angew. Chem. Int. Ed. Engl.* **1984**, 23, 272.
- [34] See ref. [6], p. 35.
- [35] *CRC Handbook of Chemistry and Physics*, 81st ed. (Ed.: D. R. Lide), CRC Press, Boca Raton, **2000**, pp. 9–17 (geom.) and 9–55 (diss. energy).
- [36] J. W. Ochterski, G. A. Petersson, K. B. Wiberg, *J. Am. Chem. Soc.* **1995**, 117, 11299.
- [37] P. J. Bruna, G. A. Di Labio, J. S. Wright, *J. Phys. Chem.* **1992**, 96, 6269.
- [38] I. Demachy, F. Volatron, *J. Phys. Chem.* **1994**, 98, 10728.
- [39] J. Koput, *J. Mol. Spectrosc.* **1986**, 115, 438.
- [40] R. F. W. Bader, *Atoms in Molecules. A Quantum Theory*, Clarendon Press, Oxford, **1990**.
- [41] M. Lein, G. Frenking in *Theory and Applications of Computational Chemistry: The First 40 Years* (Eds.: C. E. Dykstra, K. S. Kim, G. Frenking, G. E. Scuseria), Elsevier, Amsterdam, in press.
- [42] D. F. McMillen, D. M. Golden, *Ann. Pharm. Belg. Ann. Rev. Phys. Chem.* **1982**, 33, 493.
- [43] a) J. L. Lyman, *J. Phys. Chem. Ref. Data*, **1989**, 18, 799; b) J. Berkowitz, P. M. Dehmer, W. A. Chupka, *J. Chem. Phys.* **1973**, 59, 925.
- [44] D. D. Danielson, J. V. Patton, K. Hedberg, *J. Am. Chem. Soc.* **1977**, 99, 6484.
- [45] M. M. Gilbert, G. Gundersen, K. Hedberg, *J. Chem. Phys.* **1972**, 56, 1691.
- [46] R. H. Jackson, *J. Chem. Soc.* **1962**, 4585.
- [47] C. R. Brundle, M. B. Robin, N. A. Kuebler, H. Basch, *J. Am. Chem. Soc.* **1972**, 94, 1451.
- [48] The correlation between hybridization and electronegativity is known as Bent's rule: H. A. Bent, *Chem. Rev.* **1961**, 61, 275.
- [49] J. R. Durig, Z. Shen, *J. Phys. Chem. A* **1997**, 101, 5010.
- [50] A. P. Rendell, T. J. Lee, *J. Chem. Phys.* **1994**, 101, 400.
- [51] M. Peric, B. Ostojic, B. Engels, *J. Mol. Spectrosc.* **1997**, 182, 295.
- [52] B. Ruscic, J. Berkowitz, *J. Chem. Phys.* **1991**, 95, 4378.
- [53] C. Jouany, J. C. Barthelat, J. P. Daudey, *Chem. Phys. Lett.* **1987**, 136, 52.
- [54] J. Demaison, F. Hegelund, H. Burger, *J. Mol. Struct.* **1997**, 413, 447.
- [55] M. Kaupp, B. Metz, H. Stoll, *Angew. Chem.* **2000**, 112, 4780; *Angew. Chem. Int. Ed.* **2000**, 39, 4607.
- [56] A. Ricca, C. W. Bauschlicher, Jr., *J. Phys. Chem. A* **1999**, 103, 11121.
- [57] P. von R. Schleyer, M. Kaupp, F. Hampel, M. Bremer, K. Mislow, *J. Am. Chem. Soc.* **1992**, 114, 6791.
- [58] P. Pyykkö, *Chem. Rev.* **1988**, 88, 563.

Received: May 26, 2004

Revised: November 18, 2004

Published online: January 25, 2005